Efficient Drug Delivery and Induction of Apoptosis in Colorectal Tumors Using a Death Receptor 5-Targeted Nanomedicine

Daniela Schmid[1,2], Francois Fay[1,2,3], Donna M Small[1], Jakub Jaworski[1], Joel S Riley[2], Diana Tegazzini[1], Cathy Fenning[2], David S Jones[1], Patrick G Johnston[2], Daniel B Longley[2] and Christopher J Scott[1,2]

[1]School of Pharmacy, Queen's University Belfast, Belfast, UK; [2]Centre for Cancer Research and Cell Biology, Queen's University Belfast, Belfast, UK; [3]Current address: Translational and Molecular Imaging Institute, Icahn School of Medicine at Mount Sinai, New York, New York, USA

Death Receptor 5 (DR5) is a pro-apoptotic cell-surface receptor that is a potential therapeutic target in cancer. Despite the potency of DR5-targeting agents in preclinical models, the translation of these effects into the clinic remains disappointing. Herein, we report an alternative approach to exploiting DR5 tumor expression using antibody-targeted, chemotherapy-loaded nanoparticles. We describe the development of an optimized polymer-based nanotherapeutic incorporating both a functionalized polyethylene glycol (PEG) layer and targeting antibodies to limit premature phagocytic clearance whilst enabling targeting of DR5-expressing tumor cells. Using the HCT116 colorectal cancer model, we show that following binding to DR5, the nanoparticles activate caspase 8, enhancing the anti-tumor activity of the camptothecin payload both *in vitro* and *in vivo*. Importantly, the combination of nanoparticle-induced DR5 clustering with camptothecin delivery overcomes resistance to DR5-induced apoptosis caused by loss of BAX or overexpression of anti-apoptotic FLIP. This novel approach may improve the clinical activity of DR5-targeted therapeutics while increasing tumor-specific delivery of systemically toxic chemotherapeutics.

Received 7 March 2014; accepted 9 July 2014; advance online publication 9 September 2014. doi:10.1038/mt.2014.137

INTRODUCTION

DR5 is a type I transmembrane protein belonging to the Tumor Necrosis Factor Receptor (TNFR) family. DR5, like other TNFRs, preassembles as receptor oligomers within the cell membrane via a preligand assembly domain.[1] Binding of its cognate trimeric ligand, TNF-related apoptosis-inducing ligand (TRAIL) induces higher order clustering of DR5 that triggers the recruitment of the adaptor molecule Fas-associated death domain and procaspase 8 to the cytoplasmic death domain of the receptor.[2,3] The formation of this Death-Inducing Signaling Complex (DISC) results in homo-dimerization and activation of caspase 8, which can directly activate downstream caspases in "type I" cells or cleave the Bcl-2 family member BID, resulting in activation of BAX and induction of mitochondrial-dependent apoptosis in "type II" cells.[4]

DR5 has been proposed as a therapeutic target in various solid cancers,[5] and we have previously reported that patients with stage II and stage III colorectal tumors express significantly higher levels of DR5 compared to normal colon tissue; however, colorectal tumors also overexpress the endogenous caspase 8 inhibitor FLIP, a major mediator of resistance to DR5-induced apoptosis.[6] DR5-specific agonistic antibodies such as conatumumab have been developed to target diseases such as metastatic colorectal cancer,[7,8] and promising effects in preclinical studies as a single agent and in combination with various chemotherapies including the topoisomerase I inhibitor irinotecan have been observed.[5,9] However, to date, conatumumab and other DR5 agonists have failed to demonstrate convincing efficacy in clinical trials. This is thought to be a consequence of weak DR5 activation through insufficient receptor clustering in patients and/or intrinsic resistance to death receptor-initiated apoptosis.[7,8,10]

Previously, we have shown *in vitro* that the conjugation of agonistic antibodies targeting TNFR family members on the surface of polymeric nanoparticles (NP) results in enhanced avidity and potently induces receptor activation.[11,12] In an effort to overcome some of the current issues with targeting DR5 using antibody-based therapies, we have examined their potential in a novel antibody-conjugate platform. Here, we describe the development and evaluation of DR5-targeted and camptothecin (CPT)-loaded poly(lactic-co-glycolic) acid (PLGA) NPs optimized for *in vivo* application. The NPs were engineered to include both a "stealth" hydrophilic PEG corona to minimize phagocytosis in addition to DR5-specific antibodies to target tumor cells and induce apoptosis. We demonstrate the pro-apoptotic effects of the platform *in vivo* using HCT116 adenocarcinoma xenografts and reveal that this novel nanomedicine has the potential to overcome frequent DR5 resistance mechanisms in colorectal cancer, namely loss of BAX expression and overexpression of FLIP.

RESULTS

Synthesis and characterization of antibody-targeted PEGylated PLGA NPs

Uniform NP populations were prepared using single emulsion evaporation with COOH-PEG$_{3400}$-PLGA copolymer at 25% (w/w) blended with PLGA RG502H (**Figure 1a** and **Table 1**). The exposed

The last two authors contributed equally to this work.

Correspondence: *Christopher J Scott, School of Pharmacy, Queen's University Belfast, 97 Lisburn Road, Belfast, BT9 7BL, UK. E-mail: c.scott@qub.ac.uk*

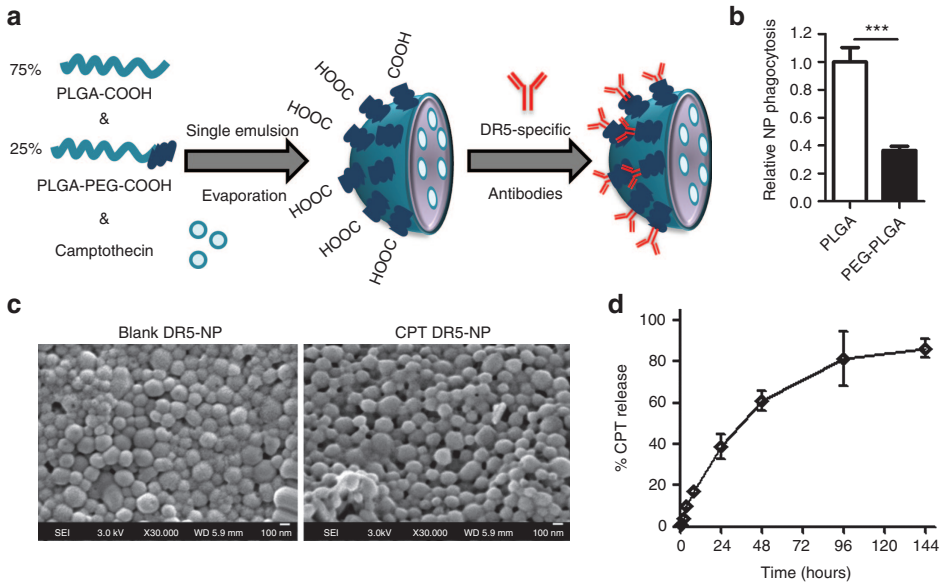

Figure 1 Preparation and characterization of DR5-targeted and CPT-loaded PEGylated PLGA NPs. (**a**) Schematic overview of the preparation process of CPT DR5-NPs. (**b**) Relative phagocytosis of fluorescent DR5-targeted PLGA and PEG-PLGA NPs after incubation with murine Raw 264.7 cells for 1 hour, mean ± SD ($n = 3$). (**c**) SEM images of blank and high content CPT DR5-NPs. (**d**) Cumulative release of CPT from high content NPs using dialysis against 50% serum in PBS at 37 °C, mean ± SD ($n = 4$). ***$P < 0.001$.

Table 1 Characterization of NPs with/without CPT loading before/after surface modification with DR5-specific antibody

	Blank nude NP	Blank DR5-NP	CPT nude NP	CPT DR5-NP
Diameter (nm)[a]	178 ± 8	217 ± 29	208 ± 8	223 ± 10
Polydispersity index[a]	0.05 ± 0.02	0.13 ± 0.03	0.15 ± 0.02	0.20 ± 0.04
Zeta potential (mV)[a]	−4.0 ± 1.0	−2.2 ± 0.8	−2.2 ± 0.3	−2.0 ± 0.6
High content CPT NP μg/mg polymer (% Entrapment efficiency)	N/A	N/A	18 ± 3 (54 ± 9)	
Low content CPT NP μg/mg polymer (% Entrapment efficiency)	N/A	N/A	3.4 ± 0.6 (68 ± 12)	

Mean ± SD ($n = 4$–6).
[a]Measured in PBS.

carboxyl groups on the surface deriving from the functionalized copolymer allowed subsequent conjugation of the DR5-specific antibody conatumumab via free amino groups within the antibody chain, using carbodiimide chemistry (16.6 ± 4.2 μg per mg NP). Furthermore, the presence of the PEG corona significantly inhibited phagocytosis by murine macrophages (**Figure 1b**). For drug-loaded NP preparations, CPT was mixed with the polymer in the organic phase before emulsification. As observed previously, the inclusion of CPT in the formulation increased the size and heterogeneity of the NP population.[12] Similarly, increases of NP size distribution were obtained for DR5-NPs due to the conjugation of high molecular weight antibodies to the NP surface (**Table 1**). Further confirmation of the size distribution (~200 nm) of blank and CPT-loaded DR5-NPs was obtained by scanning electron microscopy (SEM) (**Figure 1c**). Finally, the controlled release profile of the drug from the particles was monitored in PBS containing 50% serum at 37 °C, where a cumulative release of the compound was observed over a period of 6 days (**Figure 1d**).

DR5-NPs initiate apoptosis

The ability of the DR5-NPs to bind to colon adenocarcinoma HCT116 cells was next examined. Confocal microscopy using NPs formulated with a fluorescently labeled PLGA firstly revealed that DR5 targeting enhanced the binding of the NPs to the cells. DR5 costaining revealed broad distribution of DR5 throughout the cells and some colocalization with DR5-NPs, which was not evident with nude NPs; indicating that the antibody-conjugated NPs could bind to DR5 on the cells (**Figure 2a**). To confirm this interaction more conclusively, Western blot analysis of the protein complexes interacting with the NPs was performed. This showed that the DR5-NPs (but not the nude or IgG control NPs) were bound to DR5 in a complex with caspase 8 (**Figure 2b**). Caspase 8 was present in this complex predominantly in its cleaved p41/43-forms, but also in its p18-form indicative of its dimerization and activation at the DR5 DISC. Fully processed p18-caspase 8 can remain bound at the DISC or be released into the cytoplasm,[13] explaining its presence in both the supernatant and precipitated fraction. In agreement with the observed recruitment and processing of procaspase 8, enzymatic activity assays confirmed significantly increased levels of both caspase 8 and executioner caspases 3/7 following treatment with DR5-NPs (**Figure 2c**). Control NPs and free anti-DR5 antibody were incapable of inducing this effect. The enhanced receptor activation induced by DR5-NPs over free antibody is the consequence of the simultaneous presentation

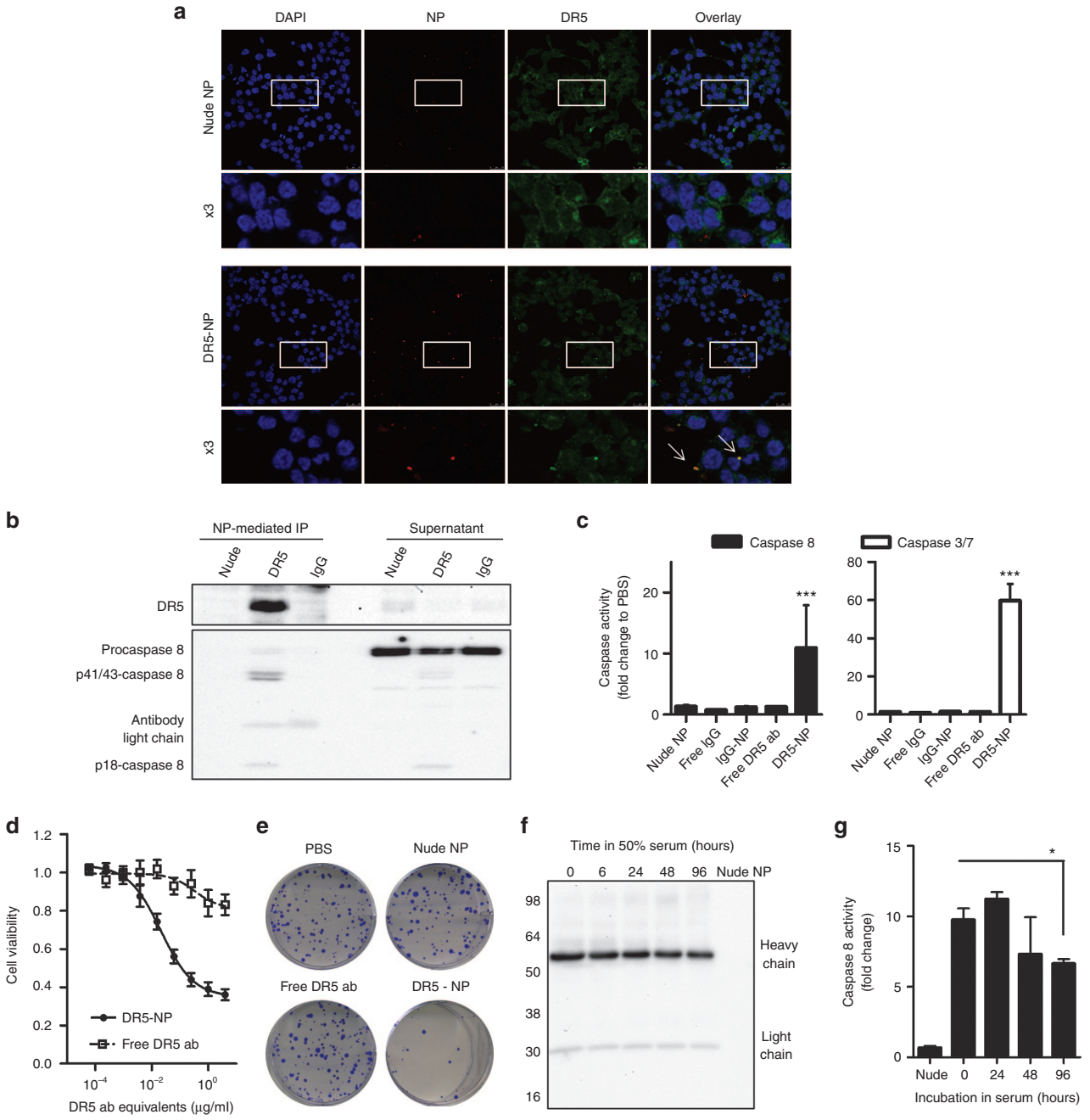

Figure 2 DR5-NPs initiate extrinsic apoptosis in HCT116 colorectal cancer cells. (**a**) Confocal microscopy images of cells treated with nude or DR5-NPs (0.2 mg/ml) for 1 hour; cell nucleus in blue, NPs in red and DR5 in green; the white arrows highlight colocalization in yellow. (**b**) Western blot analysis of DR5 and caspase 8 in the precipitate and supernatant following treatment of live cells for 2 hours and subsequent NP-mediated immunoprecipitation (IP). (**c**) Caspase 8 and 3/7 activity following treatment with DR5-NPs (0.2 mg/ml) or appropriate controls for 6 hours, mean ± SD (n = 3). (**d**) Dose-response curves of DR5-NPs and free anti-DR5 antibody (ab) after 48 hours of incubation, mean ± SEM, n = 3 (free) and 4 (DR5-NPs). (**e**) Reduction of colony formation following treatment with DR5-NPs (0.1 mg/ml) or controls for 1 hour and subsequent incubation for 12 d. (**f**) Western blot analysis of humanized DR5-specific antibody remaining on the NP surface following incubation in 50% serum at 37 °C for the indicated time. (**g**) Caspase 8 activity in HCT116 cells following treatment with DR5-NPs (0.2 mg/ml) for 6 hours after preincubation in 50% serum at 37 °C for the indicated time, mean ± SD (n = 3). *P < 0.05. ***P < 0.001.

of multiple binding paratopes on the NP surface that efficiently induces DR5 clustering and DISC formation. Furthermore, in a competition assay, caspase 8 activity was significantly reduced when the cells were preincubated with excess free DR5-specific antibody (**Supplementary Figure S1a**), further highlighting the specificity of this interaction.

The impact of NP-mediated DR5 clustering on cell viability was next assessed using MTT assays, which revealed that DR5-NPs induce a more pronounced cytotoxic effect than free antibody (**Figure 2d**). Moreover, colony formation was clearly reduced after only 1 hour of incubation with DR5-NPs, whereas free antibody did not impact on clonogenic survival (**Figure 2e**).

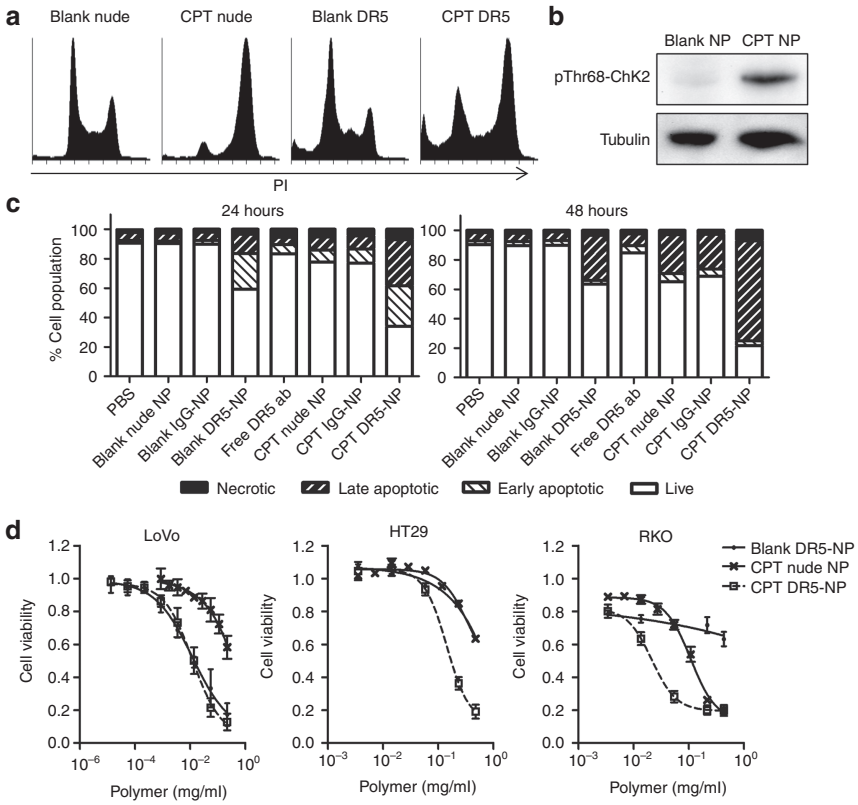

Figure 3 CPT loading enhances apoptosis induced by DR5-NPs in colorectal cancer cells. (**a**) Cell cycle analysis in HCT116 cells using RNase A/PI staining and flow cytometry following NP treatment (0.05 mg/ml) for 24 hours. (**b**) Western blot analysis of phosphorylated Chk2 (pThr68-Chk2) following treatment of HCT116 cells with NPs (0.02 mg/ml) for 24 hours. (**c**) Annexin V/PI staining after treatment of HCT116 cells with 0.10 or 0.05 mg/ml NPs and appropriate controls for 24 or 48 hours respectively, (n = 3); live: double negative; early apoptotic: annexin V positive; necrotic: PI positive; late apoptotic: double positive. (**d**) Dose-response curves of LoVo, HT29 and RKO colorectal cancer cell lines after treatment with NPs for 24 hours, mean ± SD, (n = 3).

The observed pro-apoptotic effect was DR5-dependent as shown by receptor silencing using siRNA (**Supplementary Figure S1b,c**). Furthermore, normal colon fibroblasts (CCD-18Co), which express low levels of DR5, are significantly less sensitive to DR5-NPs than HCT116 tumor cells (**Supplementary Figure S2**). Finally, we assessed the stability of the DR5-NPs following incubation in 50% serum at 37 °C. This demonstrated that the antibody remained on the NP surface up to 96 hours (**Figure 2f**) and that within this timeframe, the NPs maintained their ability to significantly activate caspase 8 (**Figure 2g**).

CPT loading enhances apoptosis induced by DR5-NPs

Next, we investigated the potential of exploiting this targeted NP formulation as a carrier for the chemotherapeutic drug CPT. Incubation with CPT-loaded NPs caused S- and G2/M-arrest within 24 hours indicative of CPT-induced DNA damage (**Figure 3a**). Furthermore, it was shown that CPT loading induced Thr68-phosphorylation of Chk2 (pThr68-Chk2) (**Figure 3b**); Chk2 is an upstream kinase activated by ATM in response to DNA double-strand breaks such as those caused by topoisomerase-I inhibition.[14,15] Apoptotic cell death was detected by flow cytometry in 40% of the cells 24 hours after treatment with DR5-NPs, and this was enhanced to 70% when CPT was loaded into the NP core (**Figure 3c**). This effect increased to 80% by 48 hours, with the vast majority exhibiting a late stage apoptotic phenotype. Notably, the extent of apoptosis induced by the blank DR5-NPs did not increase between 24 and 48 hours, further highlighting the additional effects that were induced by encapsulated CPT. The effects of CPT DR5-NPs were also investigated in other colorectal cancer cell lines. The LoVo metastatic colorectal cancer cell line is highly sensitive to DR5-NP-mediated cell death and CPT does not further enhance this effect, whereas the TRAIL-resistant RKO and HT29 cell lines[16] were markedly sensitized to DR5-mediated cell death through the codelivery of CPT (**Figure 3d**). Blank NPs had no effect on cell viability at the applied polymer concentrations (**Supplementary Figure S3**).

DR5-targeting potentiates the anti-tumor effects of CPT

The therapeutic effects of DR5-NPs were next evaluated *in vivo* using athymic mice bearing HCT116 xenografts. The tumor volume was reduced by ~35% in mice treated with DR5-NPs over both PBS and control-IgG conjugated NPs by day 22 following five serial treatments. These effects were comparable to the freely administered anti-DR5 antibody without significant weight loss during the time of treatment (**Figure 4a,b**). The effectiveness of the antibody, free or NP-bound, was clearly evident through immunohistochemical staining of cleaved caspase 3, highlighting the ability of the antibody to initiate apoptosis in both these treatment groups (**Figure 4c**). It has recently been shown that free

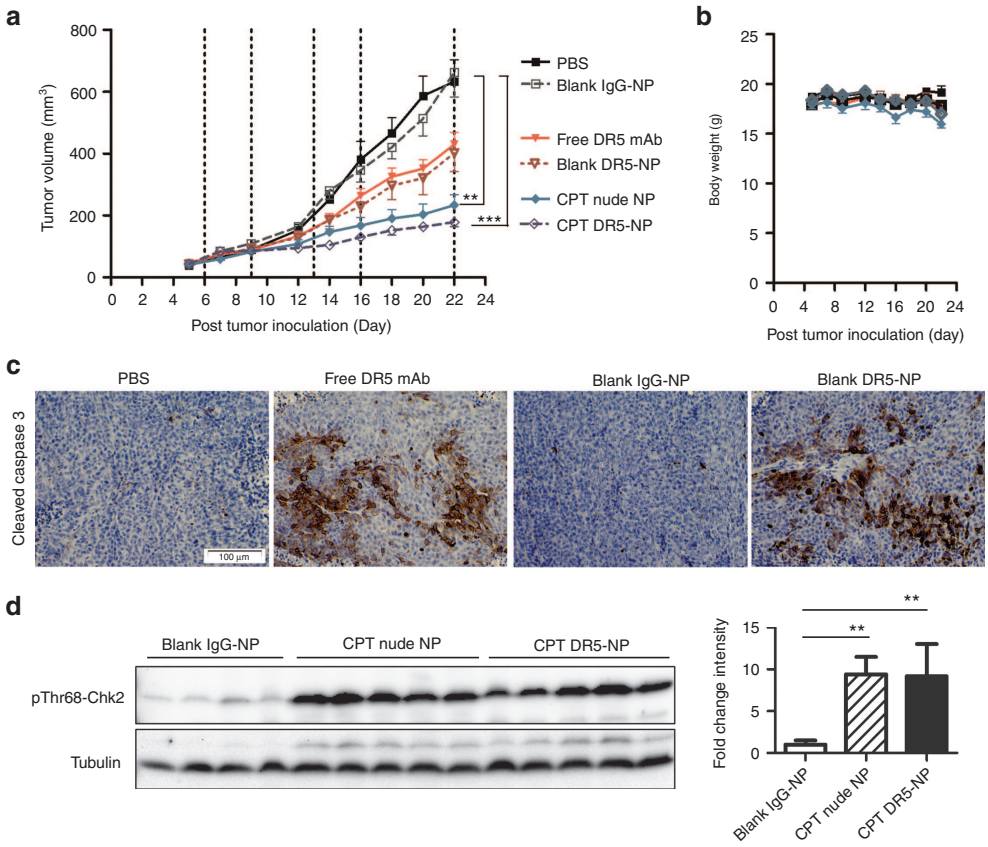

Figure 4 DR5-targeting potentiates the anti-tumor effects of CPT in HCT116 xenografts. (**a**) Tumor volume in Balb/c nude mice, dashed lines indicate the time points of treatment with PBS, NP formulations or free anti-DR5 antibody (1.7 mg/kg DR5-specific antibody, 1.9 mg/kg CPT), mean ± SEM, (n = 8–10). (**b**) Body weight, mean ± SEM (n = 4–5). (**c**) Images of paraffin-embedded tumor tissue excised on day 23 and stained for cleaved caspase 3, ×10 magnification. (**d**) Western blot analysis of pThr68-Chk2 in lysates of individual tumors excised on day 23; corresponding densitometry shown in the right panel, mean ± SD (n = 4–5). $^{**}P < 0.01$. $^{***}P < 0.001$.

DR5-targeted antibodies are cross-linked through Fcγ receptors (FcγR) that are found on a range of immune cells[17–19] and therefore, it was not unexpected that free anti-DR5 antibodies exhibited activity in murine tumor models. The therapeutic effects generated by inclusion of CPT in the NP formulations were also assessed. At the study end point, tumor growth was significantly inhibited by 65% following serial administration of CPT nude NPs, and this anti-tumor activity was further enhanced when the NPs were coated with DR5-targeting antibodies inhibiting tumor growth by 74% (**Figure 4a**). To determine whether NP-delivered CPT induced DNA damage, the tumor lysates were analyzed for pThr68-Chk2. Significant increases in pThr68-Chk2 were observed in tumors from animals treated with CPT nude NPs and CPT DR5-NPs compared to tumors from blank IgG-NP treated mice (**Figure 4d**). Collectively, these results demonstrate that both active pharmaceutical ingredients of the nanoconjugate have produced therapeutic effects *in vivo* and that the combination of CPT encapsulated in DR5-NPs yields superior antitumor activity.

DR5-NPs overcome BAX deficiency in combination with CPT

Intrinsic resistance of tumors toward DR5-mediated apoptosis may be the major factor limiting the clinical utility of DR5-targeting agonists and explain the relatively disappointing results of the clinical trials of these agents that have been reported to date.[10] Loss of BAX expression is frequently observed in microsatellite unstable colorectal cancer,[20] and we have previously reported that BAX null HCT116 cells are resistant to TRAIL-induced apoptosis.[21] Hence, we examined the potential of CPT DR5-NPs to overcome apoptosis resistance in BAX null HCT116 cells.[22] As HCT116 are type II cells,[21] DR5-mediated apoptosis is dependent on amplification of caspase activity via the intrinsic mitochondria-regulated apoptotic pathway, and as anticipated, the absence of BAX rendered these cells insensitive to DR5-NPs, as shown by the lack of cleaved PARP (lane 7, **Figure 5a**). Initial treatments of these cells with CPT DR5-NPs *in vitro* produced no therapeutic effect, but a preincubation with a sub-lethal concentration of free CPT was found to sensitize the BAX null cells to DR5 agonism, as indicated by PARP cleavage (lane 8, **Figure 5a**). Interestingly, we observed that these effects were concomitant with a reduction in the levels of the anti-apoptotic caspase inhibitor XIAP.[23] Birinapant is a small molecule that antagonizes inhibitors of apoptosis (IAPs) including XIAP,[24] and the pretreatment with this small molecule inhibitor sensitized the resistant BAX null cells to DR5-NP-mediated apoptosis (**Figure 5b**); similar effects were observed using an XIAP-targeted siRNA (**Supplementary Figure S4**). The effects caused by birinapant were not as dramatic as observed following pretreatment with CPT (**Supplementary**

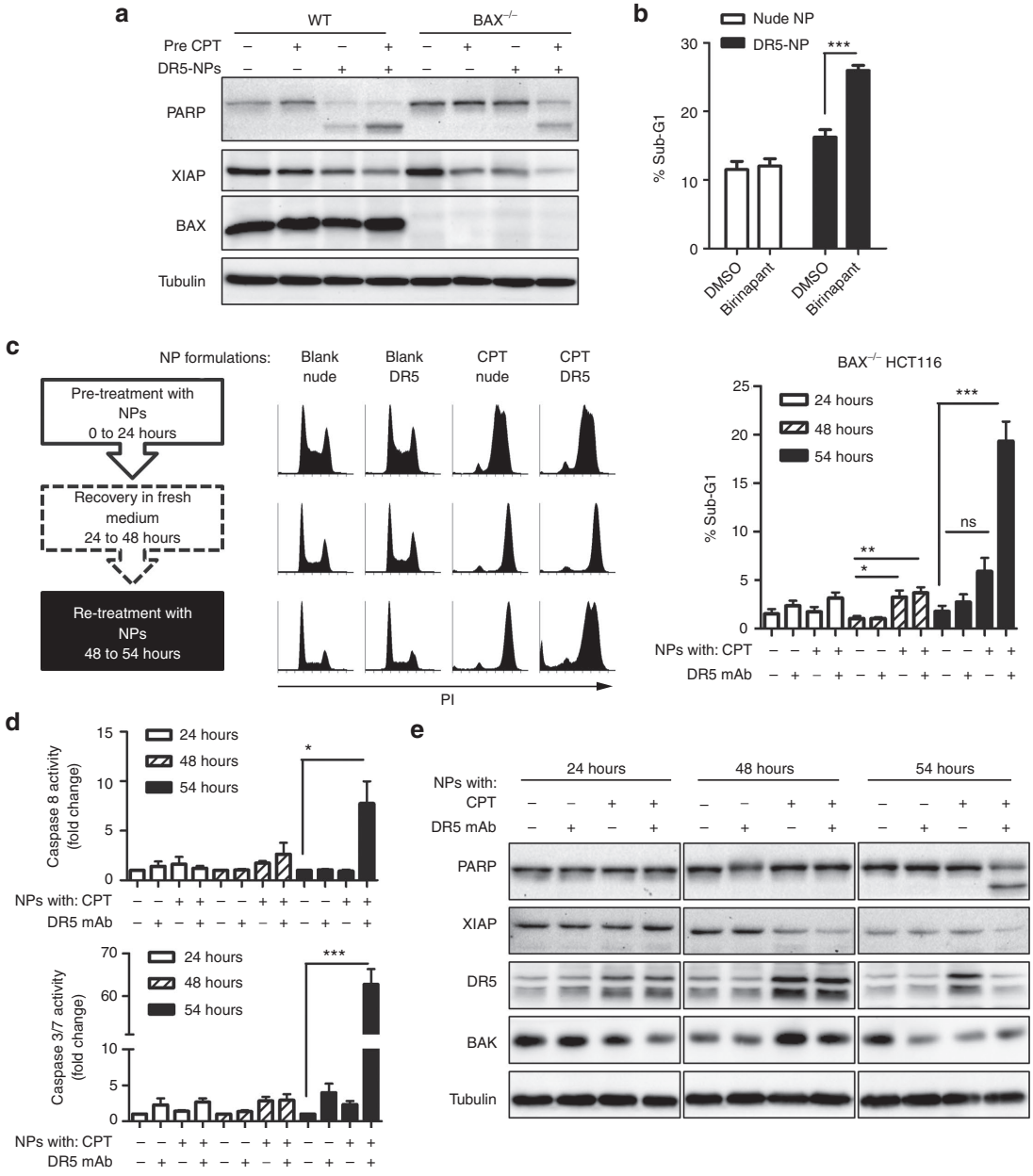

Figure 5 DR5-NPs overcome BAX deficiency in HCT116 cells in combination with CPT. (**a**) Western blot analysis of PARP, XIAP, and BAX in wild-type (WT) and BAX$^{-/-}$ HCT116 cells following pretreatment with CPT (Pre CPT, 0.1 µmol/l) for 16 hours and subsequent treatment with DR5-NPs (0.05 mg/ml) for 6 hours. (**b**) Quantification of apoptotic (sub-G1) cell populations analyzed by RNase A/PI staining and flow cytometry following treatment with birinapant (1 µmol/l) for 1 hour and subsequent treatment with DR5-NPs (0.05 mg/ml) for 6 hours; mean ± SD (n = 3). (**c**) RNase A/PI staining and flow cytometry analysis of BAX$^{-/-}$ HCT116 cells following serial NP treatment (0.01 mg/ml) as outlined in the flow chart; quantification of the sub-G1 cell populations in the right panel, mean ± SD (n = 4). (**d**) Caspase 8 and 3/7 activity following the treatment regime; mean ± SD (n = 3). (**e**) Western blot analysis of PARP, XIAP, DR5 and BAK in BAX$^{-/-}$ HCT116 cells following the treatment regime. *P < 0.05, **P < 0.01, and ***P < 0.001.

Figure S5), suggesting that other molecular events favoring cell death are induced by CPT, such as upregulation of DR5 cell surface expression, which was detected following CPT treatment (**Supplementary Figure S6**).

On the basis of these findings, a sequential treatment strategy was designed for treating Bax null cells with CPT DR5-NPs (and associated controls) as outlined in **Figure 5c**. Induction of cell cycle arrest and onset of apoptosis in the cells was examined by flow cytometry. Following the initial 24 hours treatment with CPT loaded NPs, cell cycle arrest in S- and G2/M-phases was apparent, but none of the treatment groups induced cell death as indicated by a lack of cells in the sub-G1 phase (**Figure 5c**, 24 hours). The CPT-induced G2/M-arrest was more pronounced after subsequent incubation in fresh medium for a further 24 hours and a small cell population (~4%) underwent cell death (**Figure 5c**, 48 hours). However, after re-treatment for only 6 hours, the CPT DR5-NPs induced a significant increase in cell death, whereas the other NP treatment groups were unable to induce significant effects compared to cells treated with blank nude NPs (**Figure 5c**, 54 hours). This corresponded with

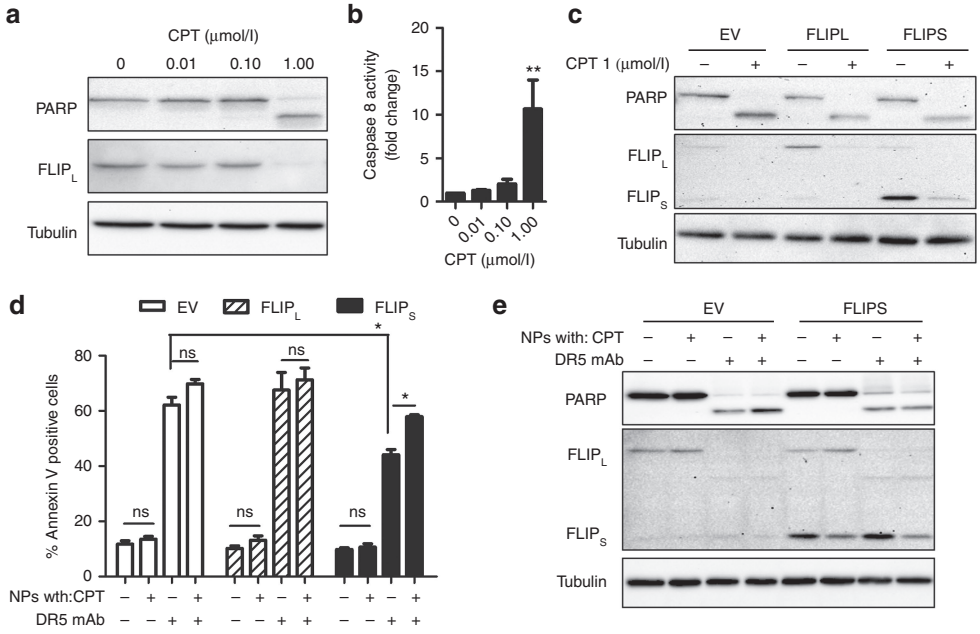

Figure 6 DR5-NPs overcome high FLIP levels in HCT116 cells with enhanced effects in combination with CPT. (**a**) Western blot analysis of PARP and FLIP$_L$ following treatment with free CPT for 24 hours. (**b**) Caspase 8 activation following treatment with free CPT for 24 hours, mean ± SD (n = 3). (**c**) Western blot analysis of PARP and FLIP in FLIP$_L$, FLIP$_S$ and empty vector (EV) transduced HCT116 cells following treatment with free CPT (1 μmol/l) for 24 hours. (**d**) Annexin V binding in FLIP$_L$, FLIP$_S$ and EV transduced cells following treatment with NPs (0.05 mg/ml) for 12 hours, mean ± SD (n = 3). (**e**) Western blot analysis of PARP and FLIP in FLIP$_S$ and EV transduced cells following treatment with NPs (0.05 mg/ml) for 12 hours. *P < 0.05 and **P < 0.01.

significantly increased activation of caspase 8 and caspases 3/7 (**Figure 5d**), and PARP cleavage (**Figure 5e**). Further protein analysis also revealed that DR5 was upregulated 24 hours following treatment with CPT loaded NPs, and this effect was enhanced after 48 hours, the point of retreatment. At this time-point, and consistent with earlier results (**Figure 5a**), XIAP was downregulated in cells treated with CPT loaded NPs. Upon retreatment of the cells with the CPT DR5-NPs, DR5 expression was decreased (**Figure 5e**); this is most likely due to receptor internalization and lysosomal degradation as proposed by Austin *et al.*[25] We also analyzed levels of BAK, which functions similarly to BAX by forming pores in the outer mitochondrial membrane during apoptosis.[26] Small alterations in BAK levels were observed but these did not correlate with the enhanced induction of apoptosis with CPT DR5-NPs. Taken together, these results demonstrate that repeated treatments with CPT DR5-NPs are able to overcome apoptotic resistance in colorectal cancer cells caused by the absence of BAX through downregulation of XIAP and simultaneous upregulation of DR5.

DR5-NPs overcome apoptosis resistance mediated by FLIP

Another major resistance mechanism to DR5-initiated apoptosis is upregulation of FLIP, which is an endogenous inhibitor of caspase 8 and can cause resistance to DR5-mediated apoptosis.[27] FLIP is found overexpressed in tissues of a range of malignancies including colorectal carcinoma.[6,28,29] First, we examined the impact of CPT treatment on endogenous FLIP proteins in wild-type HCT116 cells. Treatment with a concentration of CPT (1 μmol/l) that induced PARP cleavage within 24 hours markedly downregulated FLIP long (FLIP$_L$) levels (**Figure 6a**). This effect was accompanied by increasing activity of caspase 8 with ascending CPT concentrations, which reached significance at the highest CPT concentration (**Figure 6b**). As no decrease in FLIP mRNA levels were observed in cells treated with 1 μmol/l CPT for 24 hours (**Supplementary Figure S7**), these results suggest that FLIP is degraded following treatment with this concentration of CPT, resulting in activation of caspase 8. To investigate the effect of FLIP overexpression on DR5-NP–induced apoptosis and the potential to overcome this resistance mechanism by codelivery of CPT, we investigated HCT116 cells that overexpress the two main FLIP splice isoforms; FLIP$_L$ and FLIP short (FLIP$_S$). Similar to the observations with endogenous protein, both exogenous splice variants were downregulated following CPT treatment, and this correlated with PARP cleavage (**Figure 6c**). Notably, overexpression of FLIP$_L$ did not impact on the ability of DR5-NPs to induce apoptosis following treatment with DR5-NPs (**Figure 6d**). In contrast, FLIP$_S$ overexpression reduced apoptosis, however, the impact of FLIP$_S$ overexpression was significantly less when CPT was encapsulated into DR5-NPs; this reflects the downregulation of exogenous FLIP$_S$ in response to treatment with both CPT-loaded NP formulations (**Figure 6e**). The differential effects observed in the two FLIP overexpressing cell lines are most likely due to the different expression levels of the two exogenous FLIP proteins with FLIP$_S$ overexpressed ~4 times more highly (**Figure 6c**), and reflected by the observation that FLIP$_S$ overexpression was very effective at blocking apoptosis induced by cotreatment with recombinant human TRAIL (rhTRAIL) and CPT (**Supplementary Figure S8**). These results demonstrate that DR5-NPs can activate the extrinsic apoptotic pathway despite moderate (FLIP$_L$ model) and high

($FLIP_S$ model) overexpression of FLIP, and this effect is further enhanced by codelivery of CPT.

DISCUSSION

In this work, we have developed a polymeric NP drug delivery system suitable for *in vivo* application that incorporates an antibody therapeutic targeting DR5 and chemotherapy payload. The therapeutic effectiveness of this modality was validated *in vivo*, and moreover, we showed that common resistance mechanisms to DR5-initiated apoptosis could be overcome by this approach.

We have previously examined the conjugation of antibodies to the surface of PLGA-based NPs to elicit improved uptake in tumor cell populations *in vitro.*[11,12] PLGA is a biodegradable and biocompatible polymer approved in various medical applications.[30] However, these polymeric NPs are hydrophobic and once in circulation, serum proteins can rapidly aggregate on the surface of such hydrophobic nanomaterials promoting macrophage uptake.[31] The inclusion of a surface layer of hydrophilic polymers such as PEG can counteract macrophage uptake and reduce the rapid NP clearance that occurs in the organs of the mononuclear phagocyte system.[32] This has been shown to therefore enhance the half-life of PEGylated PLGA-based NPs.[33,34] Here, we successfully incorporated a carboxyl-functionalized PEG_{3400} into the formulation and, in agreement with previous studies, found that macrophage uptake of the NPs was diminished.

The conjugation of a DR5-targeting antibody to the surface of these NPs was shown to promote binding to the target receptor and induce formation of the apoptosis-inducing DR5 DISC. Although the presentation of the DR5 antibody on the surface of the NP significantly increased apoptosis compared to free antibody *in vitro*, this differential effect was not evident *in vivo*. It is well characterized that the free anti-DR5 antibody with only two paratopes is inefficient at promoting higher-order clustering and activation of DR5 in cell-based assays.[9] However, once applied in murine *in vivo* studies, it does achieve agonistic activity comparable to DR5-NPs. This phenomenon is dependent on FcγR engagement of the antibody on myeloid cells which facilitates multiple paratope presentation that in turn drives receptor activation on the surface of the tumor cells.[17–19] The clinical significance of this effect in patients remains poorly characterized, and FcγR polymorphisms affecting antibody affinity may dictate the effectiveness of the drug.[8,35] However, this issue is circumvented by our novel approach of using NPs to present multiple paratopes to drive DR5 activation on the surface of tumor cells.

Considering the physiological role of TRAIL/DR5 in tumor immune surveillance,[36] it is not surprising that many cancer cells develop resistance mechanisms in order to escape destruction mediated by TRAIL-expressing immune cells.[10] We hypothesized that efficient receptor crosslinking through DR5-NPs, in combination with the delivery of a cytotoxic agent, may enhance DR5-mediated apoptosis and more importantly help to overcome frequently occurring resistance mechanisms in cancer cells. CPT was selected as the cargo chemotherapy in this approach but issues with its solubility, stability and toxicity profile have led to the development and clinical application of derivatives, namely irinotecan and topotecan.[37] However, the promising clinical results of CRLX101, a polymeric nano-formulation of CPT currently investigated in clinical phase II trials, clearly highlight the therapeutic potential of this highly potent compound when delivered appropriately.[38] CPT NPs exhibited significant anti-tumor effects in HCT116 xenografts that were markedly enhanced when the NPs were functionalized with DR5 antibody; this is consistent with the results of combination studies of conatumumab with irinotecan *in vitro* and *in vivo*.[9] The HCT116 tumors proved highly sensitive to the levels of CPT encapsulated in the NPs, and this may have partially masked the therapeutic advantage of the conjugated DR5 antibodies. Nonetheless, the results obtained from the DR5-targeted NP groups clearly show that the conjugates were able to localize to the tumor and initiate apoptosis. Given that this antibody does not cross-react with murine DR5, future studies will require a species-matched agonistic antibody in order to undertake detailed biodistribution and pharmacokinetic analyses; examining parameters such as particle size, antibody orientation and use of antibody fragments to optimize the pro-apoptotic effects and evaluate the ability of the antibodies to enhance targeting of the NP to tumors.

Another key consideration in resistance of tumors to extrinsic apoptosis is the requirement for mitochondrial amplification of an extrinsic apoptotic signal, which determines whether cells are classified as type I (not required) and type II cells (required).[10] The deregulation of proteins within the mitochondrial pathway through overexpression of anti-apoptotic Bcl-2[39] and Bcl-X_L[40] or loss of BAX protein,[22] which commonly occur in human malignancies,[41] renders type II cells resistant to extrinsic apoptosis. Therefore, we investigated whether CPT-loaded DR5-NPs could overcome the resistance of BAX-deficient type II HCT116 cells to DR5-mediated apoptosis. Pretreatment with CPT-loaded NPs increased DR5 expression in the BAX-deficient cells and also caused a marked downregulation of XIAP. XIAP is the only IAP that directly inhibits caspases, binding with high affinity to effector caspases 3/7 and initiator caspase 9, and is recognized as a critical inhibitor of death receptor-induced apoptosis.[42] Importantly, serial treatments with CPT-loaded, but not blank DR5-NPs, overcame resistance to TRAIL-induced apoptosis in BAX null cells. Mechanistically, this is most likely a result of simultaneous upregulation of DR5 and downregulation of XIAP. This is in agreement with previous work showing that chemo-sensitization of BAX null HCT116 cells to TRAIL-mediated apoptosis was a consequence of p53-mediated upregulation of DR5[43] and our own work showing that resistance of BAX null cells to TRAIL-induced apoptosis can be overcome by downregulating XIAP.[21]

FLIP is a key regulator of death receptor-mediated apoptosis and is found overexpressed in a range of malignancies.[6,28,29,44] High expression of FLIP is proposed to contribute to resistance to death receptor-targeted therapy by disrupting procaspase 8 homo-dimerization and activation at the DISC.[10,27] The results presented herein indicate that the enhanced receptor oligomerization induced by DR5-NPs can overcome FLIP-mediated resistance to DR5-induced apoptosis when FLIP is overexpressed at moderate levels ($FLIP_L$ model). Moreover, even in cells with high levels of FLIP expression ($FLIP_S$ model), DR5-NPs induced high levels of apoptosis, and these cells could be further sensitized through incorporation of CPT into the NP core, as codelivery

of CPT resulted in FLIP downregulation. Taken together, these results highlight the potential of this DR5-targeted platform to overcome these resistance mechanisms.

Given the recent advances in clinical application of polymer-based nanotherapeutics[38,45,46] and promising results with antibody drug conjugates (ADCs) such as Trastuzumab emtansine (T-DM1),[47] therapies that bring together anti-cancer drugs in a single therapeutic entity represent exciting new approaches for the treatment of cancer. In this study we have demonstrated the therapeutic potential of using drug-loaded, tumor-targeted NPs as an alternative ADC strategy.

MATERIALS AND METHODS

NP synthesis. NPs were prepared by single emulsion evaporation with 25% (w/w) of COOH-PEG-PLGA copolymer (see **Supplementary Materials and Methods** for polymer synthesis) mixed with PLGA RG502H (Evonik Industries, Germany). The polymer (20 mg) was dissolved in 1 ml of dichloromethane and injected into the aqueous phase (7 ml) containing 2.5% (w/v) polyvinyl alcohol in MES buffer (50 mmol/l, pH 5.0) to provide optimal conditions for downstream antibody conjugation. Emulsification was achieved by pulsary sonication on ice for 90 seconds and the resulting emulsion was stirred overnight to allow the organic solvent to evaporate. Fluorescently labeled NPs were generated by addition of 0.1% (w/w) rhodamine 6G (Sigma-Aldrich, UK) into the organic phase for macrophage uptake studies or by use of rhodamine B-conjugated PLGA (AV11, Akina, West Lafayette, IN) for confocal microscopy. (S)-(+)-CPT (Sigma-Aldrich) NPs were generated by the addition of the drug into the organic phase whereas the amount varied depending on the application (0.50% or 3.33% (w/w) for *in vitro* or *in vivo* respectively). The NPs were purified in MES buffer by 3 wash-spin cycles and conatumumab (provided by Amgen) was attached similarly to a method described previously.[11,12] Free carboxyl groups on the NP surface were activated in MES buffer with 2 mmol/l 1-Ethyl-3-(3-dimethylaminopropyl)carbodiimide (EDC) and 14 mmol/l N-Hydroxysuccinimide (NHS) for 20 minutes, centrifuged at 20,000*g* and conatumumab or control human IgG (Life Technologies, UK; 50 µg per mg of polymer) was incubated for 1 hour under stirring. NPs were washed once in PBS for removal of unbound antibody. The characterization of the nanoparticles is described in the **Supplementary Materials and Methods**.

Cell culture. The HCT116 wild-type and $Bax^{-/-}$ mutant cell lines were kindly provided by Professor Bert Vogelstein (Johns Hopkins University) and cultured in McCoy 5A medium supplemented with 10% FBS. HCT116 cell lines overexpressing $FLIP_S$ and $FLIP_L$ were generated as described previously.[48] The Raw 264.7, RKO and HT-29 cells were obtained from ATCC, LoVo cells from ECACC and maintained in supplemented DMEM.

NP uptake analysis. Raw 264.7 cells were incubated with 0.1 mg/ml of rhodamine 6G-loaded NPs for 1 hour and washed with PBS (2×), stripping buffer (50 mmol/l glycine, 150 mmol/l NaCl, pH3) and PBS (1×) before PE fluorescence was analyzed by flow cytometry. For confocal microscopy, the cells were incubated with rhodamine B-labeled NPs (0.2 mg/ml) for 1 hour and then washed in PBS (3×), stripping buffer (1×) and PBS (3×). The cells were fixed using 4% paraformaldehyde followed by further washing steps in PBS (3×). DR5 was stained using anti-DR5 antibody (1:200, Cell Signaling Technologies, Danvers, MA) and Alexa Fluor 488 donkey anti-rabbit antibody (1:200, Life Technologies). The cover slips were sealed with Prolong Gold Antifade reagent containing DAPI (Life Technologies) and the cells imaged using the Leica SP5 Confocal Microscope (×63 lens zoomed ×1–4 with a 1,024 × 1,024 frame and 400 Hz scanning speed). The analysis was carried out using Leica LAS AF software using standardized settings and exposure times.

NP-mediated IP. HCT116 cells were seeded into P90 plates and treated with 0.5 mg/ml of nude, DR5-NPs or human IgG-NPs for 2 hours, the supernatant was removed and the cells washed once in PBS. The cells were lysed at 4 °C for 15 minutes in IP lysis buffer (150 mmol/l NaCl, 20 mmol/l Tris–HCl, pH7.4, containing 0.2% NP-40, 10% glycerol) and centrifuged for 10 minutes at 4 °C at 20,000*g* to precipitate NPs with the attached proteins. The supernatant was collected and the remaining precipitate washed once in lysis buffer and separated by centrifugation before denaturation. 40% of the precipitated protein and 2% of the supernatant were subject to western blot analysis using anti-caspase 8 (1:5,000, Enzo Life Sciences, UK) and anti-DR5 antibody (1:1,000, Cell Signaling Technologies).

Assessment of apoptotic cell death. Cells were seeded in P90, 6-, 12-, or 96-well plates. Cell viability was assessed by MTT reagent (Sigma-Aldrich, UK) and data presented relative to PBS-treated cells. Caspase activity was analyzed in cell lysates (5 µg of protein) by Caspase-Glo 3/7 or 8 assays (Promega, UK) and the data expressed as fold change to control cells. Cell cycle progression was analyzed by PI staining and flow cytometry after cell fixation and RNase A (Qiagen, UK) digestion. Expression of phosphatidyl serine was analyzed by annexin V-FITC/PI staining following Logue *et al.*[49] RhTRAIL was obtained from Merck Millipore, UK, birinapant from TetraLogic Pharmaceutical (Malvern, PA). Silencing of XIAP and DR5 was carried out using validated siRNA and assessed by western blot and flow cytometry respectively as previously described.[21,50] For the assessment of clonogenic survival, 400 cells were seeded into six-well plates and treated for 1 hour upon adherence, the medium replaced and incubated for 12 days to allow the formation of colonies (stained with 0.4% crystal violet solution). Cell lysates were prepared with RIPA lysis buffer supplemented with protease inhibitors. Protein expression levels were assessed by Western immunoblot incubating the membrane with primary antibodies overnight at 4 °C (BAX, XIAP, pThr68-Chk2, 1:1,000, Cell Signaling Technologies; BAK, 1:1,000, Santa Cruz Biotechnology, Germany; FLIP, 1:1,000, Enzo Life Sciences; α-tubulin as loading control, 1:10,000, Abcam, UK; PARP, 1:5,000, eBioscience, UK) and secondary antibodies for 1 hour at room temperature.

HCT116 xenograft study. All *in vivo* experiments were carried out in accordance with the UK Home Office and approved by Queen's University Belfast Ethical Review Committee. 2×10^6 HCT116 cells were implanted subcutaneously onto both flanks of 9 weeks old female Balb/c nude mice (Harlan Laboratories, UK) using matrigel (BD, UK). The animals were treated intravenously via tail vein injections with 2 mg of NPs or controls (corresponding to 1.9 mg/kg CPT and 1.7 mg/kg conatumumab) when xenografts reached an average size of 60 mm^3. Tumor tissue was lysed with RIPA lysis buffer containing protease and phosphatase inhibitors using the TissueLyser LT (Qiagen, UK) and subject to Western blotting. The intensity of protein bands was determined by densitometry using Image Lab Software (BioRad, UK). Formalin-fixed tumors were paraffin-embedded, sectioned (6 µm) and stained with anti-cleaved caspase 3 antibody (1:200, Cell Signaling Technologies) according to the manufacturer's recommendation. Images were taken using an Olympus BH2 microscope at ×10 magnification.

Statistical analysis. One-way analysis of variance with Tukey's *post hoc* test or the Student's *t*-test was used to analyze statistical significance between several groups or two groups respectively. The Kruskal–Wallis test was applied to determine the statistical significance of tumor volume *in vivo*. The null hypothesis was accepted for $P \geq 0.05$ or labeled with * for $P < 0.05$, ** for $P < 0.01$ and *** for $P < 0.001$ when rejected.

SUPPLEMENTARY MATERIAL

Figure S1. Pro-apoptotic effects of DR5-NPs are DR5 dependent.
Figure S2. DR5-NPs exhibit reduced cytotoxic effects against normal colon fibroblasts.
Figure S3. Effect of blank nude NPs on cell viability of colorectal

cancer cell lines.

Figure S4. XIAP silencing enhances pro-apoptotic effect of DR5-NPs in resistant cells.

Figure S5. Combination therapies enhance cytotoxic effects of DR5-NPs against resistant HCT116 cells.

Figure S6. CPT exposure upregulates DR5 cell surface expression.

Figure S7. Assessment of FLIP mRNA levels by qPCR in HCT116 cells following treatment with free CPT for 24 hours, mean±SD (n = 3).

Figure S8. FLIP expression suppresses the pro-apoptotic activity of recombinant human (rhTRAIL).

Materials and Methods.

ACKNOWLEDGMENTS

We thank Amgen for kindly providing conatumumab and Queen's University Belfast for the studentship awarded to D.S. This work was supported by MRC Confidence in Concept funding. The authors declare no conflict of interest.

REFERENCES

1. Chan, FK (2007). Three is better than one: pre-ligand receptor assembly in the regulation of TNF receptor signaling. *Cytokine* **37**: 101–107.
2. Valley, CC, Lewis, AK, Mudaliar, DJ, Perlmutter, JD, Braun, AR, Karim, CB *et al.* (2012). Tumor necrosis factor-related apoptosis-inducing ligand (TRAIL) induces death receptor 5 networks that are highly organized. *J Biol Chem* **287**: 21265–21278.
3. Verbrugge, I, Johnstone, RW and Smyth, MJ (2010). SnapShot: Extrinsic apoptosis pathways. *Cell* **143**: 1192, 1192.e1–1192, 1192.e2.
4. Oldenhuis, CN, Stegehuis, JH, Walenkamp, AM, de Jong, S and de Vries, EG (2008). Targeting TRAIL death receptors. *Curr Opin Pharmacol* **8**: 433–439.
5. den Hollander, MW, Gietema, JA, de Jong, S, Walenkamp, AM, Reyners, AK, Oldenhuis, CN *et al.* (2013). Translating TRAIL-receptor targeting agents to the clinic. *Cancer Lett* **332**: 194–201.
6. McLornan, DP, Barrett, HL, Cummins, R, McDermott, U, McDowell, C, Conlon, SJ *et al.* (2010). Prognostic significance of TRAIL signaling molecules in stage II and III colorectal cancer. *Clin Cancer Res* **16**: 3442–3451.
7. Cohn, AL, Tabernero, J, Maurel, J, Nowara, E, Sastre, J, Chuah, BY *et al.* (2013). A randomized, placebo-controlled phase 2 study of ganitumab or conatumumab in combination with FOLFIRI for second-line treatment of mutant KRAS metastatic colorectal cancer. *Ann Oncol* **24**: 1777–1785.
8. Fuchs, CS, Fakih, M, Schwartzberg, L, Cohn, AL, Yee, L, Dreisbach, L *et al.* (2013). TRAIL receptor agonist conatumumab with modified FOLFOX6 plus bevacizumab for first-line treatment of metastatic colorectal cancer: A randomized phase 1b/2 trial. *Cancer* **119**: 4290–4298.
9. Kaplan-Lefko, PJ, Graves, JD, Zoog, SJ, Pan, Y, Wall, J, Branstetter, DG *et al.* (2010). Conatumumab, a fully human agonist antibody to death receptor 5, induces apoptosis via caspase activation in multiple tumor types. *Cancer Biol Ther* **9**: 618–631.
10. Dimberg, LY, Anderson, CK, Camidge, R, Behbakht, K, Thorburn, A and Ford, HL (2013). On the TRAIL to successful cancer therapy? Predicting and counteracting resistance against TRAIL-based therapeutics. *Oncogene* **32**: 1341–1350.
11. Fay, F, McLaughlin, KM, Small, DM, Fennell, DA, Johnston, PG, Longley, DB *et al.* (2011). Conatumumab (AMG 655) coated nanoparticles for targeted pro-apoptotic drug delivery. *Biomaterials* **32**: 8645–8653.
12. McCarron, PA, Marouf, WM, Quinn, DJ, Fay, F, Burden, RE, Olwill, SA *et al.* (2008). Antibody targeting of camptothecin-loaded PLGA nanoparticles to tumor cells. *Bioconjug Chem* **19**: 1561–1569.
13. Lavrik, I, Krueger, A, Schmitz, I, Baumann, S, Weyd, H, Krammer, PH *et al.* (2003). The active caspase-8 heterotetramer is formed at the CD95 DISC. *Cell Death Differ* **10**: 144–145.
14. Shiloh, Y (2006). The ATM-mediated DNA-damage response: taking shape. *Trends Biochem Sci* **31**: 402–410.
15. Huang, M, Miao, ZH, Zhu, H, Cai, YJ, Lu, W and Ding, J (2008). Chk1 and Chk2 are differentially involved in homologous recombination repair and cell cycle arrest in response to DNA double-strand breaks induced by camptothecins. *Mol Cancer Ther* **7**: 1440–1449.
16. Beranova, L, Pombinho, AR, Spegarova, J, Koc, M, Klanova, M, Molinsky, J *et al.* (2013). The plant alkaloid and anti-leukemia drug homoharringtonine sensitizes resistant human colorectal carcinoma cells to TRAIL-induced apoptosis via multiple mechanisms. *Apoptosis* **18**: 739–750.
17. Haynes, NM, Hawkins, ED, Li, M, McLaughlin, NM, Hämmerling, GJ, Schwendener, R *et al.* (2010). CD11c+ dendritic cells and B cells contribute to the tumoricidal activity of anti-DR5 antibody therapy in established tumors. *J Immunol* **185**: 532–541.
18. Wilson, NS, Yang, B, Yang, A, Loeser, S, Marsters, S, Lawrence, D *et al.* (2011). An Fc? receptor-dependent mechanism drives antibody-mediated target-receptor signaling in cancer cells. *Cancer Cell* **19**: 101–113.
19. Li, F and Ravetch, JV (2012). Apoptotic and antitumor activity of death receptor antibodies require inhibitory Fc? receptor engagement. *Proc Natl Acad Sci USA* **109**: 10966–10971.
20. Ouyang, H, Furukawa, T, Abe, T, Kato, Y and Horii, A (1998). The BAX gene, the promoter of apoptosis, is mutated in genetically unstable cancers of the colorectum, stomach, and endometrium. *Clin Cancer Res* **4**: 1071–1074.
21. Wilson, TR, McEwan, M, McLaughlin, K, Le Clorennec, C, Allen, WL, Fennell, DA *et al.* (2009). Combined inhibition of FLIP and XIAP induces Bax-independent apoptosis in type II colorectal cancer cells. *Oncogene* **28**: 63–72.
22. LeBlanc, H, Lawrence, D, Varfolomeev, E, Totpal, K, Morlan, J, Schow, P *et al.* (2002). Tumor-cell resistance to death receptor–induced apoptosis through mutational inactivation of the proapoptotic Bcl-2 homolog Bax. *Nat Med* **8**: 274–281.
23. Kashkar, H (2010). X-linked inhibitor of apoptosis: a chemoresistance factor or a hollow promise. *Clin Cancer Res* **16**: 4496–4502.
24. Krepler, C, Chunduru, SK, Halloran, MB, He, X, Xiao, M, Vultur, A *et al.* (2013). The novel SMAC mimetic birinapant exhibits potent activity against human melanoma cells. *Clin Cancer Res* **19**: 1784–1794.
25. Austin, CD, Lawrence, DA, Peden, AA, Varfolomeev, EE, Totpal, K, De Mazière, AM *et al.* (2006). Death-receptor activation halts clathrin-dependent endocytosis. *Proc Natl Acad Sci USA* **103**: 10283–10288.
26. Youle, RJ and Strasser, A (2008). The BCL-2 protein family: opposing activities that mediate cell death. *Nat Rev Mol Cell Biol* **9**: 47–59.
27. Safa, AR (2012). c-FLIP, a master anti-apoptotic regulator. *Exp Oncol* **34**: 176–184.
28. Valnet-Rabier, MB, Challier, B, Thiebault, S, Angonin, R, Margueritte, G, Mougin, C *et al.* (2005). c-Flip protein expression in Burkitt's lymphomas is associated with a poor clinical outcome. *Br J Haematol* **128**: 767–773.
29. McCourt, C, Maxwell, P, Mazzucchelli, R, Montironi, R, Scarpelli, M, Salto-Tellez, M *et al.* (2012). Elevation of c-FLIP in castrate-resistant prostate cancer antagonizes therapeutic response to androgen receptor-targeted therapy. *Clin Cancer Res* **18**: 3822–3833.
30. Lü, JM, Wang, X, Marin-Muller, C, Wang, H, Lin, PH, Yao, Q *et al.* (2009). Current advances in research and clinical applications of PLGA-based nanotechnology. *Expert Rev Mol Diagn* **9**: 325–341.
31. Walkey, CD, Olsen, JB, Guo, H, Emili, A and Chan, WC (2012). Nanoparticle size and surface chemistry determine serum protein adsorption and macrophage uptake. *J Am Chem Soc* **134**: 2139–2147.
32. Perry, JL, Reuter, KG, Kai, MP, Herlihy, KP, Jones, SW, Luft, JC *et al.* (2012). PEGylated PRINT nanoparticles: the impact of PEG density on protein binding, macrophage association, biodistribution, and pharmacokinetics. *Nano Lett* **12**: 5304–5310.
33. Li, Y, Pei, Y, Zhang, X, Gu, Z, Zhou, Z, Yuan, W *et al.* (2001). PEGylated PLGA nanoparticles as protein carriers: synthesis, preparation and biodistribution in rats. *J Control Release* **71**: 203–211.
34. Khalil, NM, do Nascimento, TC, Casa, DM, Dalmolin, LF, de Mattos, AC, Hoss, I *et al.* (2013). Pharmacokinetics of curcumin-loaded PLGA and PLGA-PEG blend nanoparticles after oral administration in rats. *Colloids Surf B Biointerfaces* **101**: 353–360.
35. Pan, Y, Haddad, V, Sabin, T, Baker, N, Hei, YJ, Galimi, F *et al.* (2011). Predictive value of Fc gamma receptor IIIa genotype in response to conatumumab in three phase II studies. *J Clin Oncol* **29(15_suppl)**: Abstract 3103.
36. Cretney, E, Takeda, K, Yagita, H, Glaccum, M, Peschon, JJ and Smyth, MJ (2002). Increased susceptibility to tumor initiation and metastasis in TNF-related apoptosis-inducing ligand-deficient mice. *J Immunol* **168**: 1356–1361.
37. Pommier, Y (2006). Topoisomerase I inhibitors: camptothecins and beyond. *Nat Rev Cancer* **6**: 789–802.
38. Weiss, GJ, Chao, J, Neidhart, JD, Ramanathan, RK, Bassett, D, Neidhart, JA *et al.* (2013). First-in-human phase 1/2a trial of CRLX101, a cyclodextrin-containing polymer-camptothecin nanopharmaceutical in patients with advanced solid tumor malignancies. *Invest New Drugs* **31**: 986–1000.
39. Fulda, S, Meyer, E and Debatin, KM (2002). Inhibition of TRAIL-induced apoptosis by Bcl-2 overexpression. *Oncogene* **21**: 2283–2294.
40. Hinz, S, Trauzold, A, Boenicke, L, Sandberg, C, Beckmann, S, Bayer, E *et al.* (2000). Bcl-XL protects pancreatic adenocarcinoma cells against CD95- and TRAIL-receptor-mediated apoptosis. *Oncogene* **19**: 5477–5486.
41. Cory, S and Adams, JM (2002). The Bcl2 family: regulators of the cellular life-or-death switch. *Nat Rev Cancer* **2**: 647–656.
42. Eckelman, BP, Salvesen, GS and Scott, FL (2006). Human inhibitor of apoptosis proteins: why XIAP is the black sheep of the family. *EMBO Rep* **7**: 988–994.
43. Wang, S and El-Deiry, WS (2003). Requirement of p53 targets in chemosensitization of colonic carcinoma to death ligand therapy. *Proc Natl Acad Sci USA* **100**: 15095–15100.
44. Shirley, S and Micheau, O (2013). Targeting c-FLIP in cancer. *Cancer Lett* **332**: 141–150.
45. Hrkach, J, Von Hoff, D, Mukkaram Ali, M, Andrianova, E, Auer, J, Campbell, T *et al.* (2012). Preclinical development and clinical translation of a PSMA-targeted docetaxel nanoparticle with a differentiated pharmacological profile. *Sci Transl Med* **4**: 128ra39.
46. Hamaguchi, T, Doi, T, Eguchi-Nakajima, T, Kato, K, Yamada, Y, Shimada, Y *et al.* (2010). Phase I study of NK012, a novel SN-38-incorporating micellar nanoparticle, in adult patients with solid tumors. *Clin Cancer Res* **16**: 5058–5066.
47. Zolot, RS, Basu, S and Million, RP (2013). Antibody-drug conjugates. *Nat Rev Drug Discov* **12**: 259–260.
48. Hurwitz, JL, Stasik, I, Kerr, EM, Holohan, C, Redmond, KM, McLaughlin, KM *et al.* (2012). Vorinostat/SAHA-induced apoptosis in malignant mesothelioma is FLIP/caspase 8-dependent and HR23B-independent. *Eur J Cancer* **48**: 1096–1107.
49. Logue, SE, Elgendy, M and Martin, SJ (2009). Expression, purification and use of recombinant annexin V for the detection of apoptotic cells. *Nat Protoc* **4**: 1383–1395.
50. Abdelghany, SM, Schmid, D, Deacon, J, Jaworski, J, Fay, F, McLaughlin, KM *et al.* (2013). Enhanced antitumor activity of the photosensitizer meso-Tetra(N-methyl-4-pyridyl) porphine tetra tosylate through encapsulation in antibody-targeted chitosan/alginate nanoparticles. *Biomacromolecules* **14**: 302–310.